JOURNAL OF MATERIALS SCIENCE **38** (2003) 3121–3129

Monte Carlo simulation of creep failure in a 0°/90° plain weave SiC/SiC composite lamina

D. N. COON
Mechanical Engineering Department, University of Wyoming, Laramie, WY 82071
E-mail: dcoon@uwyo.edu

A Monte Carlo model of the effects of fiber creep in a 0°/90° plain weave ceramic-grade Nicalon reinforced SiC composite has been developed. Creep degradation of fibers was predicted to result in stress dependent premature failure of woven ceramic matrix composites, and that premature failure was modeled using a power-law. A power-law exponent of 3.1 ± 0.1 was predicted. The power-law exponent was predicted to be independent of initial crack size for crack length to specimen width ratios of 0.02, 0.10, 0.25, and 0.50. The power-law exponent was also predicted to be independent of the matrix to fiber strength ratio for ratios from 0.25 to 1.0. Premature failure in the 90° (transverse) tows resulted in premature failure of the composite for low values of the matrix to fiber strength ratio (less than 0.75), and decreased creep life was predicted for decreased matrix to fiber strength ratio. For a matrix to fiber strength ratio of 1.0, the creep life of the woven composite was predicted to be equivalent to a unidirectional composite. At small initial crack lengths, a 10% improvement in the creep life was predicted for a reduction in the matrix to fiber strength ratio from 1.0 to 0.75. This improvement was related to the formation of microcracks in the 90° tows and shielding of the macrocrack tip from accelerated creep damage. This improvement in the predicted creep life at a matrix to fiber strength ratio of 0.75 was predicted to be independent of applied stress. However, improvement of the creep life was not predicted to occur for larger values of initial crack length.

1. Background

The long-term reliability of ceramic matrix composites in load-bearing, high temperature applications has been a concern. Stress dependent premature failure of ceramic matrix composites has been observed at elevated temperature [1–27], and several degradation mechanisms have been identified including creep [1–14], fiber/environment reaction [15–25], wear of fiber surfaces during cyclic loading [26], and subcritical crack growth within individual fibers [27]. An understanding of degradation of individual fibers on the resulting composite behavior has been identified [3, 8, 12–14] as a critical need in improving the performance of these materials.

Creep damage in ceramic matrix composites loaded in tension initiated with a single macrocrack growing in the direction perpendicular to the maximum principal stress [15]. Some fibers remained intact and bridged the macrocrack. Catastrophic failure of tension specimens was preceded by fiber pullout, and then fiber failure.

Damage accumulation in woven SiC reinforced ceramic matrix composites initiated with microcrack formation around processing pores [28]. Next, cracks were observed to propagate in 90° (transverse) fiber tows. After crack formation in 90° fiber tows, cracks were observed to form in 0° (longitudinal) fiber tows. Catastrophic failure resulted from the propagation of a macrocrack through the microcracked composite.

The influence of fiber degradation by creep and the stress dependent premature failure of single tow SiC mini-composites have been modeled with Monte Carlo Simulation [12–14]. For axially loaded mini-composites, damage accumulation began with nucleation of a matrix crack, and continued with the formation of bridging fibers during extension of that matrix crack. Failure of bridging fibers due to creep degradation of those fibers resulted in continued extension of the matrix crack, and transition to a fully cracked, fiber dominated system. Continued creep degradation of remaining fibers led to catastrophic failure of the mini-composite. A power-law was used to model the stress dependent premature failure of ceramic-grade Nicalon fiber reinforced SiC mini-composites, and a power-law exponent of 3.01 ± 0.06 was predicted. The predicted power-law exponent agrees reasonably well with experimental studies of SiC fiber reinforced mini-composites [3]. A transition to rapid degradation of the mini-composite was predicted after only about 10% of the fibers exhibited significant creep damage [12–14].

The effect of a variety of fiber characteristics on the predicted creep response of a SiC mini-composite has been reported [14]. High fracture toughness, high fiber strength, high Weibull parameter, small fibers, and large

fiber volume fraction were predicted to improve the creep life of SiC mini-composites.

The purpose of this communication is to report a Monte Carlo model of stress dependent premature failure a 0°/90° plain weave ceramic-grade Nicalon fiber reinforced SiC composite lamina resulting from creep degradation of fibers.

2. Description of Monte Carlo model

The geometry of the composite system modeled in this communication is shown in Fig. 1. The geometry consisted a of a 0°/90° plain weave, ceramic-grade Nicalon fiber reinforced SiC composite containing an edge macrocrack loaded in Mode I [29]. The model described in this communication predicts the behavior of a single lamina of the geometry shown in Fig. 1. The composite lamina was modeled as small volumes of material each containing either a 0° fiber tow element (longitudinal mini-composite element with fibers parallel to applied stress) or a 90° fiber tow element (transverse minicomposite element with fibers perpendicular to applied stress). The cross section of each mini-composite element was a square with unit dimension equal to the width of a single fiber tow. The macrocrack length to specimen width (a/w) ratio was varied while maintaining a constant number, 25, of elements co-linear with the macrocrack tip.

A flow chart of the Monte Carlo model described in this communication is shown in Fig. 2. The input to the model included creep behavior of fiber reinforced ceramic matrix mini-composites, applied stress, initial crack length, and position of the initial crack tip. The model used numerical results of the creep

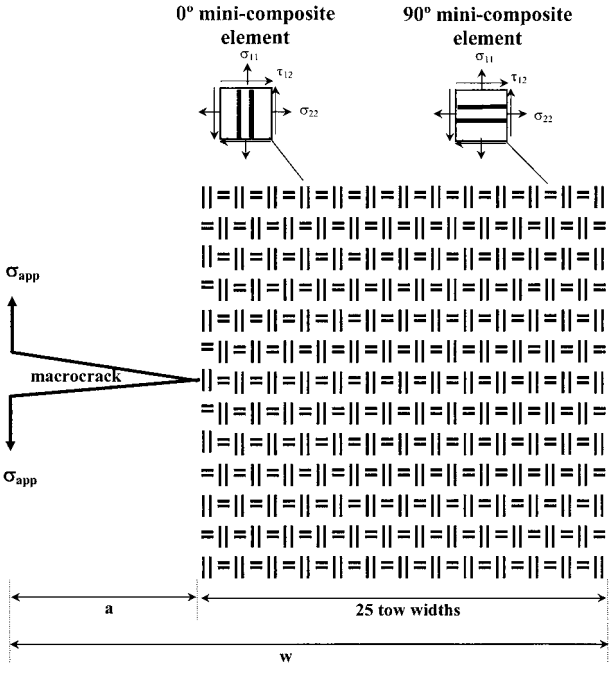

Figure 1 Schematic representation of woven composite architecture modeled in this study. Mini-composite elements containing fibers oriented parallel to the applied stress were defined as 0° mini-composite elements, and mini-composite elements containing fiber oriented perpendicular to the applied stress were defined as 90° mini-composite elements.

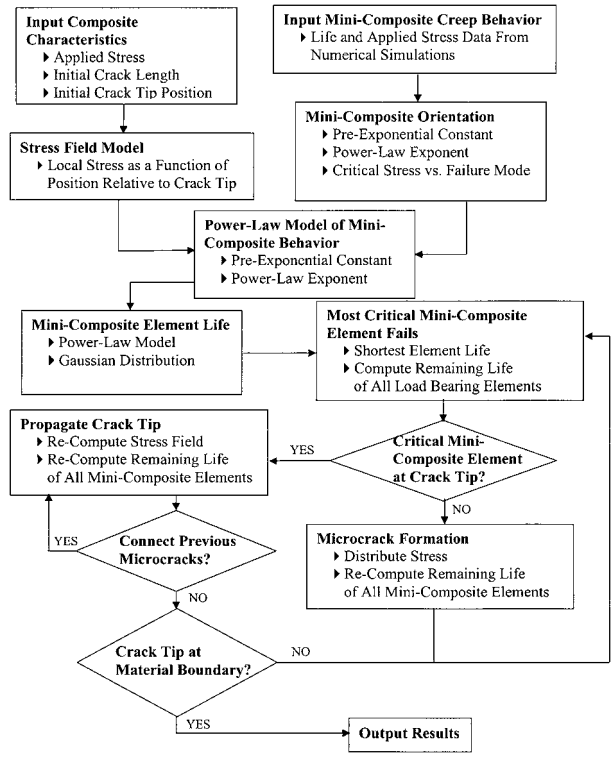

Figure 2 Flowchart of Monte Carlo model of creep of fibers in a woven ceramic matrix composite lamina described in this study.

behavior of ceramic-grade Nicalon fiber reinforced SiC matrix mini-composites [14]. Mini-composite behavior has been reported to consist of a complex set of stress dependent responses resulting from creep rupture of individual fibers. The complex set of stress dependent responses included initiation of microcrack growth within the mini-composite, quasi-static microcrack extension through the mini-composite, and finally failure of individual fibers in a system described as a fully bridged microcrack. Fiber bridging and creep rupture of bridging fibers was included in the mini-composite behavior.

The physical parameters of the Monte Carlo model described in this communication included the applied stress, initial macrocrack length, the position of the macrocrack, and the ratio of the matrix strength to the fiber strength. The initial macrocrack length to specimen width ratio was used as a measure of the initial macrocrack length. As an example, an initial macrocrack length to specimen width ratio of 0.02 was equivalent to an initial macrocrack length of approximately 1 mini-composite element width (Fig. 1). An initial macrocrack length to specimen width ratio of 0.10 was equivalent to an initial macrocrack length of approximately 5 mini-composite element widths. An initial macrocrack length to specimen width ratio of 0.25 was equivalent to approximately 17 mini-composite element widths.

The Monte Carlo model described in this communication used a power-law model to describe mini-composite behavior [14]. In this manner, the behavior of a mini-composite element under any loading condition could be predicted from knowledge of the local stress state in the mini-composite element. The well-known Linear Elastic Fracture Mechanics solution [29] to the

TABLE I Potential failures in elements containing either 0° or 90° fiber tows

Failure type	Fiber tow orientation	Corresponding LEFM stress term
Tensile fiber failure	0°	σ_{11}
Shear interface failure	0°	τ_{12}
Tensile matrix failure	0°	σ_{22}
Tensile fiber failure	90°	σ_{22}
Shear interface failure	90°	τ_{12}
Tensile matrix failure	90°	σ_{11}

stress field in material containing an edge-crack loaded in Mode I loading was used to model the local stress state in each mini-composite element of the composite lamina. A scaling factor was used to avoid any numerical problems with the singularity at the macrocrack tip [29]. The Linear Elastic Fracture Mechanics solution was used to describe the effect of applied stress, macrocrack length, and proximity to the macrocrack tip on the local stress state in each mini-composite element. The predicted response of each mini-composite element was, however, dependent on the orientation of the fibers in the mini-composite element.

Three types of potential element failure were hypothesized for each mini-composite element orientation (Table I). The time for each failure type to occur by creep rupture of individual fibers was predicted, and the shortest predicted time was used as the predicted creep response of that mini-composite element. Prediction of the shortest failure time for each mini-composite element was accomplished by comparing the local stress state in that mini-composite element to the required critical stress state in that mini-composite element according to:

$$t_f = 1 + A\left(\sigma_{\text{local}}^{-n} - \sigma_{\text{crit}}^{-n}\right) \tag{1}$$

where t_f = predicted creep lifetime, A = pre-exponential power-law constant, σ_{local} = local stress, σ_{crit} = critical stress (stress resulting in failure in 1 time unit), and n = power-law exponent.

For simplicity, it was assumed that the power-law exponent was independent of the failure mode (approximately 3 [14]), and the pre-exponential power-law constant was computed as necessary. The critical stresses for rapid failure of mini-composite elements are given in Table II. The critical stress for fiber failure in tension, 421 MPa, was predicted from numerical models of mini-composite behavior [14], but agree quite well with experimental studies of ceramic-grade Nicalon fiber reinforced mini-composites [3]. The critical stress for interface failure in shear, 39 MPa, was taken as the average value obtained from Iocipescu shear tests of ceramic-grade Nicalon fiber reinforced SiC composites [30]. No experimental or numerical results of the critical stress for matrix failure in tension were available from in-situ studies on composite materials. Therefore, this critical stress for matrix failure was varied systematically in the current numerical model from 25% of the value of the critical stress for fiber failure (105 MPa) to 100% of the critical value for fiber failure (421 MPa). Since both the matrix and fiber phases in the results described in this communication were SiC, low values of the critical stress for matrix failure would be consistent with a composite lamina containing processing defects or pores. High values of the critical stress for matrix failure would be consistent with a composite lamina containing no processing defects.

TABLE II Critical stress for element failure with ceramic-grade Nicalon fibers

Failure type	Critical stress value	Reference
Tensile fiber failure	421 MPa	3, 14
Shear interface failure	39 MPa	30
Tensile matrix failure	105–421 MPa	

Predicted mini-composite element behavior using Equation 1 was then a function of the constituent materials, applied stress, macrocrack length, proximity of the element to the macrocrack tip, and mini-composite orientation. Once the shortest predicted creep lifetime for each mini-composite element was identified, that lifetime was subjected to a random Gaussian variation as a means to model material variability. The average of the Gaussian variation was the predicted lifetime, and the standard deviation was 7.5% of this predicted value [13].

The incorporation of variation in the prediction of individual mini-composite element response is an important characteristic of the numerical model described in this communication. The creep behavior of individual composite specimens is known to exhibit variation [4], and power-law models of creep response predict only the average response. To predict creep responses of individual mini-composite elements, variation must be incorporated into a power-law prediction.

The lifetime of each mini-composite element containing random Gaussian variation was combined into a Monte Carlo creep life response surface for the composite lamina. This Monte Carlo creep life response surface was a function of the mini-composite behavior, mini-composite orientation, material variability, applied stress, macrocrack length, and proximity to the macrocrack tip.

The Monte Carlo creep life response surface was used to model the progression of creep damage in the 0°/90° plain weave, ceramic-grade Nicalon fiber reinforced SiC composite lamina. The mini-composite element exhibiting the minimum predicted creep life failed first. The result of mini-composite element failure was modeled as either macrocrack extension or microcrack formation in the composite lamina. Failure of an mini-composite element adjacent to the macrocrack tip was modeled as extension of the macrocrack into that mini-composite element, and force from the failed mini-composite element was distributed by re-computing the Linear Elastic Fracture Mechanics solution to the stress field. Failure of an mini-composite element not adjacent to the macrocrack tip was modeled as formation of a microcrack, and force from the failed mini-composite element was distributed to remaining elements using

an inverse square distribution law described in detail elsewhere [12–14]. In addition, the numerical model allowed macrocrack extension by connection of microcracks formed during previous creep damage.

Either macrocrack extension or microcrack formation resulted in two events. First, the lifetime of each remaining mini-composite element was scaled to incorporate creep damage accumulated in that mini-composite element up to that time. Second, the remaining creep life of each mini-composite element was recomputed in relation to the change in the local stress state in that mini-composite element, and a revised Monte Carlo creep life response surface was computed. The revised Monte Carlo creep life response surface was used to predict the next mini-composite element to fail. In this manner, the numerical model iterated to catastrophic composite lamina failure defined as extension of the macrocrack to a edge of the composite lamina. This numerical approach accounted for material variability and all accumulated creep damage in mini-composite elements. However, the model also allowed the progression of creep damage to depend on both macrocrack extension and microcrack formation. Individual solutions of the numerical model would depend on the random variation built into the Monte Carlo creep life response surface, but the average of multiple solutions would provide insight into expected composite lamina behavior.

3. Results and discussion

Typical creep damage predicted by the numerical model described in this communication is shown in Fig. 3 for an applied stress of 70 MPa, initial macrocrack length to specimen width ratio of 0.02, and a matrix to fiber strength ratio of 0.5 (critical stress for tensile failure in matrix of 210 MPa). Tensile failure of fibers was predicted to determine creep lifetime in every 0° mini-composite element. Tensile failure of the matrix was predicted to determine creep lifetime in every 90° mini-composite element. Even though failure of the interface in shear exhibited the lowest critical strength, no mini-composite element was predicted to fail by this mode due to the relatively small shear stresses predicted by Linear Elastic Fracture Mechanics solution [29]. The local stress field in each mini-composite element was dominated by the σ_{11} term, and the other terms were relatively small in comparison. In each instance, the largest stress term in the Linear Elastic Fracture Mechanics solution was predicted to be the most critical stress term and determine creep lifetime of that mini-composite element.

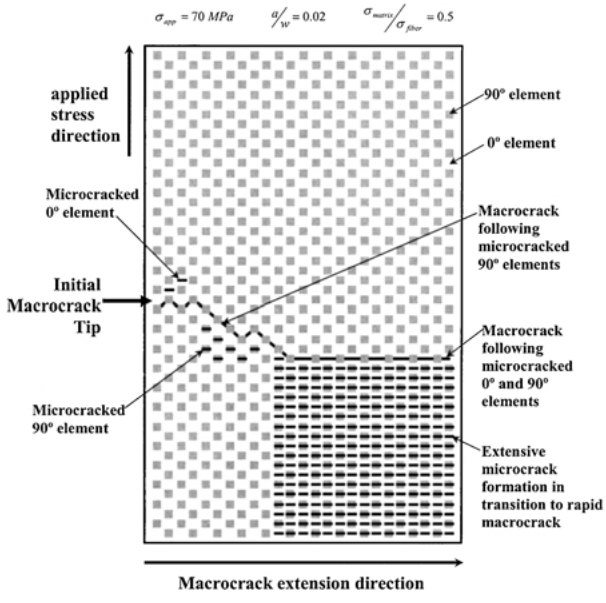

Figure 3 Typical predicted creep damage in a woven ceramic-grade Nicalon fiber reinforced ceramic matrix composite lamina. The applied stress was 70 MPa, the initial crack length to specimen width ratio was 0.02, and the matrix to fiber strength ratio was 0.5.

The lack of predicted interface failure in shear does not imply that delamination type failures often reported in experimental studies [28, 30] were not predicted to occur. Matrix failure in tension could occur in either the interior of the mini-composite element or at the surface of the mini-composite element. Matrix failure at the surface of the mini-composite element would be consistent with delamination observed experimentally in composite laminates [3–11]. However, the numerical model described in this communication suggests that delamination failures result from local tensile fields not local shear fields. The numerical model also predicted that delamination would be constrained to 90° mini-composite elements. It should be noted that fiber pullout due to fiber/matrix interface failure was fully allowed within individual mini-composite elements, and contained in the mini-composite behavior [13].

The predicted accumulation of creep damage for the solution shown in Fig. 3 initiated with failure of 90° mini-composite elements near the macrocrack tip. Secondly, macrocrack extension was predicted to occur by connection of microcracks formed in 90° mini-composite elements. A small number of microcracks in the 0° mini-composite elements near the initial macrocrack tip was also predicted. Once the macrocrack extended out of the region of significant stress concentration (approximately 40% of the distance across the composite lamina), failure of both 0° and 90° mini-composite elements well away from the macrocrack tip was predicted. Creep damage of the composite at that point was predicted to be dominated by microcrack formation due to failure of both 0° and 90° mini-composite elements. Eventually, rapid extension of the macrocrack was predicted to occur by connection of microcracks formed near the macrocrack tip.

Creep damage initially constrained to the highly stressed 90° mini-composite elements within the area of stress concentration was expected, since these mini-composite elements exhibited the lowest predicted creep lifetime. The small number of microcracks predicted in 0° mini-composite elements near the original macrocrack tip was a result of the material variability contained in the numerical model. The extensive microcrack formation predicted in both 0° and 90° mini-composite elements late in the damage accumulation process was somewhat of a surprise since the respective critical strength of the 90° mini-composite elements was only 50% of the critical strength of the 0°

mini-composite elements. Closer examination of the numerical results revealed that the extensive microcracking predicted late the creep lifetime resulted from the combination of three characteristics of the model described in this communication. First, the small gradient in this region of the Linear Elastic Fracture Mechanics stress field solution resulted in similar local stress states predicted in each mini-composite element outside the zone of significant stress concentration associated with the macrocrack. Second, the power-law function used to predict the creep lifetime response surface (Equation 1) resulted in further reducing differences in predicted creep lifetimes between 0° and 90° mini-composite elements in this region outside the zone of significant stress concentration associated with the macrocrack. Third, once a 90° mini-composite element had been predicted to fail, the strong local effect of force distribution from failed mini-composite elements during microcrack formation tended to accelerate failure of neighboring mini-composite elements irrespective of their individual orientations. This acceleration of failure of neighboring mini-composite elements becomes a self-propagating process as force distribution from sequential failures acts to concentrate the damage zone.

Microcracking in 90° mini-composite elements in woven composites has been observed experimentally [28]. The numerical model described in this communication predicts extensive microcracking in both 0° and 90° mini-composite elements late in the creep lifetime when strain energy (potential energy) is being rapidly converted to kinetic energy. A large amount of damage on the resulting fracture surfaces would be expected. Fracture surfaces in experimental studies [3–11, 28] do show significant damage, but direct observation of sub-surface microcracking in both 0° and 90° mini-composite elements has not been reported. Therefore, it is currently uncertain whether the extensive microcracking predicted in Fig. 3 is anything more than a numerical artifact.

The predicted macrocrack length as a function of the fraction of creep lifetime is shown in Fig. 4 for an applied stress of 70 MPa, initial macrocrack length to specimen width of 0.02, and matrix to fiber strength ratio of 0.5. Failure of the first mini-composite element near the original macrocrack tip occurred after about 40% of the lifetime had passed. The majority of the lifetime, approximately 80%, was comprised of accumulation of creep damage in the absence of macrocrack extension. However, during this time, formation of microcracks in 90° mini-composite elements in the region of highest stress concentration was predicted along with creep degradation of all elements in proportion to the local stress state. After approximately 80% of the lifetime had passed, slow macrocrack extension due to connection of microcracks in 90° mini-composite elements was predicted. After about 98% of the life had passed, a transition to rapid catastrophic failure was predicted. The transition to rapid macrocrack extension was predicted to occur once the macrocrack had extended a distance of approximately 10% of the composite lamina dimension. This behavior was consistent with behavior predicted for creep failure of individual mini-composites [12–14]. Extensive microcrack formation in both the 0° and 90° mini-composite elements evident in Fig. 3 occurred during the period of rapid macrocrack extension during the last 2% of the creep lifetime.

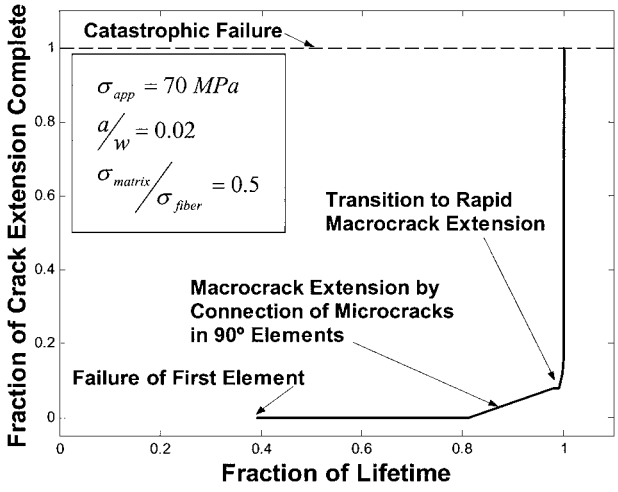

Figure 4 Typical relationship between the macrocrack crack length and time for a woven ceramic-grade Nicalon fiber reinforced SiC composite lamina for an applied stress of 70 MPa, initial macrocrack length to specimen with ratio of 0.02, and matrix to fiber strength ratio of 0.5.

The predicted creep lifetime of a 0°/90° plain weave ceramic-grade Nicalon fiber reinforced SiC composite lamina as a function of applied stress and initial macrocrack length is shown in Fig. 5. The matrix to fiber strength ratio was held constant at 0.5 for each result in Fig. 5, and 5 replicates are shown for each combination of applied stress and initial macrocrack length. The data in Fig. 5 are consistent with a stress dependent power-law response of the composite lamina due to creep of individual fibers and the resulting mini-composite failure. Both increased applied stress and increased initial macrocrack length resulted in decreased predicted creep lifetime. The predicted behavior of the composite was independent of initial macrocrack length as evidenced by parallel lines in Fig. 5.

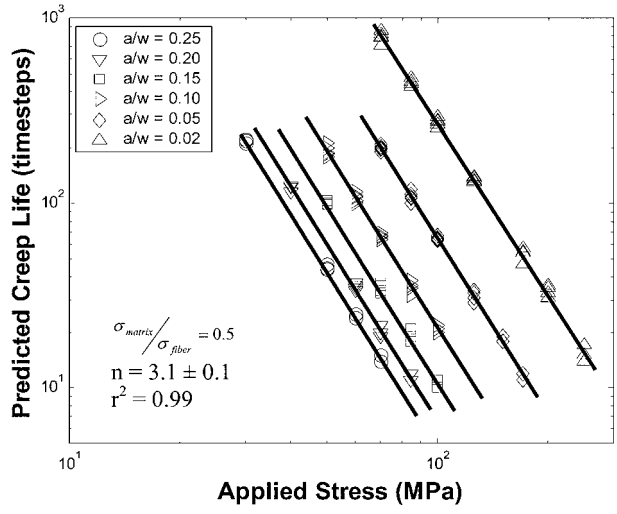

Figure 5 Predicted creep life a woven ceramic-grade Nicalon fiber reinforced SiC composite lamina as a function of applied stress and initial macrocrack length to specimen width ratio. The matrix to fiber strength ratio was 0.5 in each case, and 5 replicates were developed for each combination of applied stress and initial macrocrack length to specimen width ratio.

The data in Fig. 5 were normalized according to:

$$\frac{(t_f)}{(t)_{80\,\mathrm{MPa}}} = \left(\frac{\sigma_{\mathrm{app}}}{80\,\mathrm{MPa}}\right)^{-n} \tag{2}$$

where $(t_f)_{80\,\mathrm{MPa}}$ = predicted lifetime at an applied stress of 80 MPa and σ_{app} = applied stress.

This normalization procedure permitted the power-law exponent, n, to be determined from the combined data set. The power-law exponent was predicted to be 3.1 ± 0.1. This power-law exponent agrees reasonably well with experimental studies of woven ceramic-grade Nicalon fiber reinforced SiC composites [3–6] and with power-law exponents predicted from numerical models of mini-composites [12–14].

The effect of the matrix strength on the predicted creep response of a composite lamina is shown in Fig. 6 for an initial macrocrack length to specimen width ratio of 0.02 and matrix to fiber strength ratios of 1.0, 0.75, 0.5, and 0.25. The power-law exponent was independent of the ratio of matrix strength to fiber strength, and was computed to be 3.1 ± 0.1.

The predicted creep lifetime increased slightly when the matrix to fiber strength decreased from 1.0 to 0.75. The predicted creep lifetime of a woven composite lamina with a matrix to fiber strength ratio of 0.75 was about 10% higher than that for a woven composite lamina with a matrix to fiber strength ratio of 1.0. Further decreases in the matrix to fiber strength ratio resulted in decreased predicted creep lifetime with about a 60% reduction in predicted creep lifetime for a decrease in the matrix to fiber strength ratio from 1.0 to 0.5.

The influence of the matrix to fiber strength ratio on the predicted creep lifetime is shown in Fig. 7 a for applied stress levels of 70, 85, 100 and 125 MPa and an initial macrocrack length to specimen width of 0.02. In all cases, the predicted lifetime decreased with increased applied stress. Each data point in this plot is the average of 5 independent numerical solutions, and error bars indicate plus and minus one standard error of the mean. It should be noted that in general the error bars are smaller than the dimension of the data points, except in the case of an applied stress of 70 MPa and a matrix to fiber strength ratio of 0.81, and indicate that the numerical model provided very consistent predictions of composite lamina behavior.

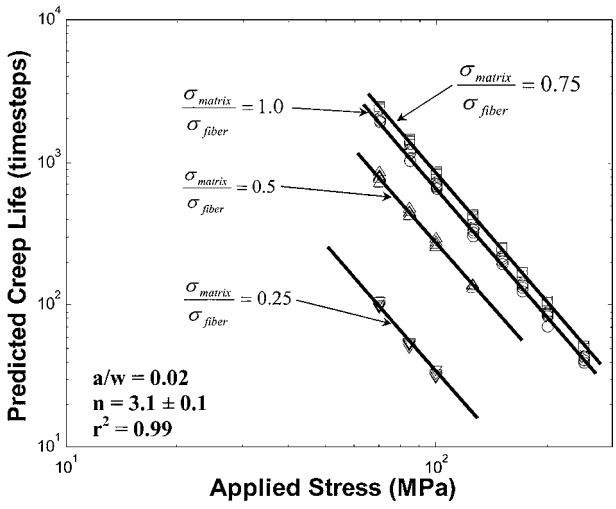

Figure 6 Predicted creep life of a woven ceramic-grade Nicalon fiber reinforced SiC composite lamina as a function of applied stress and the matrix to fiber strength ratio. The initial macrocrack length to specimen width ratio was held constant at 0.02, and 5 replicates were developed for each combination of applied stress and matrix to fiber strength ratio.

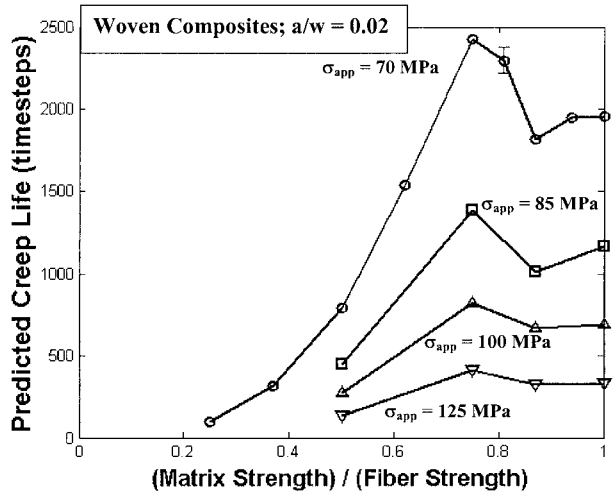

(a)

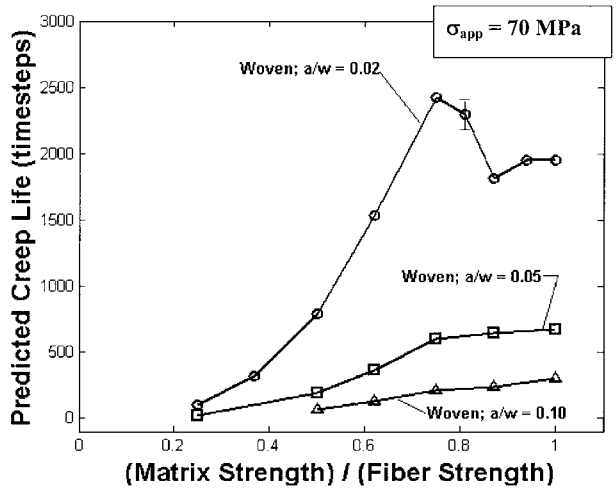

(b)

Figure 7 (a) The predicted creep life of woven ceramic-grade Nicalon fiber reinforced SiC composites as a function of the matrix to fiber strength ratio and applied stress. The initial macrocrack length to specimen width ratio was 0.02 in each case. The data points are the means of 5 replicates, and the error bars are ± one standard error of the mean. Most error bars are not visible since their dimension is less than the size of the data points. (b) The predicted creep life of woven ceramic-grade Nicalon fiber reinforced SiC composites lamina as a function of the matrix to fiber strength ratio and initial macrocrack to specimen width ratio. The applied stress was 70 MPa. The data points are the means of 5 replicates, and the error bars are ± one standard error of the mean. Most error bars are not visible since their dimension is less than the size of the data points.

At an applied stress of 70 MPa, a decrease in matrix to fiber strength ratio from 1.0 to 0.94 resulted in equivalent predicted creep lifetimes. Continued reduction of the matrix to fiber strength ratio from 0.94 to 0.87 resulted in a small decrease in the predicted creep lifetime. As the matrix to fiber strength ratio was decreased from 0.87 to 0.81, an increase in the creep lifetime was predicted. At a matrix to fiber strength ratio of 0.81, the predicted creep lifetime was about 5% higher than the predicted creep lifetime for a matrix to fiber

strength ratio of 1.0, and a modest amount of scatter in the 5 independent solutions was observed. Further decrease in the matrix to fiber strength ratio from 0.81 to 0.75 resulted in a near maximum predicted creep lifetime (about 10% higher than the corresponding result for a matrix to fiber strength ratio of 1.0). Continued decreases in the matrix to fiber strength ratio from 0.75 to 0.25 resulted in systematic decreases in the predicted creep lifetime.

At an applied stress of 85, 100, and 125 MPa, similar trends in predicted creep lifetime with decreased matrix to fiber strength ratios were observed, although the predicted creep life did decrease with increased applied stress. A maximum in the predicted creep life was observed at a matrix to fiber strength ratio of 0.75 for each level of applied stress.

The influence of the matrix to fiber strength ratio on the predicted creep lifetime for three values of initial macrocrack length to specimen width ratios and an applied stress of 70 MPa is shown in Fig. 7b. The data points are averages of 5 independent solutions, and the error bars are plus and minus one standard error of the mean. Once again, the numerical model predicted very consistent results and the length of the error bars are generally smaller than the dimension of the data point. The predicted creep lifetime decreased as the initial macrocrack length to specimen width ratio increased. A maximum in the predicted creep life at a matrix to fiber strength ratio of 0.75 was observed only for an initial macrocrack length to specimen width ratio of 0.02. A systematic decrease in predicted creep lifetime was observed for decreased matrix to fiber strength ratios for initial crack length to specimen width ratios of 0.05 and 0.10.

Comparison of Fig. 7a and b indicate that the existence of a maximum in the predicted creep life at a matrix to fiber strength ratio of 0.75 is dominated by macrocrack length rather than applied stress level. Both the applied stress and macrocrack length control the magnitude of the local stress field near the macrocrack tip. However, the applied stress primarily controlled the magnitude of the stress concentration near the macrocrack tip and the macrocrack length primarily controlled the dimension over which the significant stress concentration was observed. For small initial macrocrack lengths to specimen width ratios, a large number of the mini-composite elements were well outside the region of significant stress concentration, and exhibited very similar stress states. For large initial macrocrack length to specimen width ratios, larger numbers of mini-composite elements were within the area of significant stress concentration, and neighboring mini-composite elements exhibited dissimilar stress states.

For small initial macrocrack length to specimen width ratios, i.e. $a/w = 0.02$, and high matrix to fiber strength ratios, i.e. $\sigma_{\text{matrix}}/\sigma_{\text{fiber}} = 1.0$, the predicted creep life response surface was relatively flat outside the zone of significant stress concentration. The fiber orientation tow within each mini-composite element did not affect the predicted creep lifetime response surface. Therefore, the difference in the predicted creep lifetime of neighboring mini-composite elements was

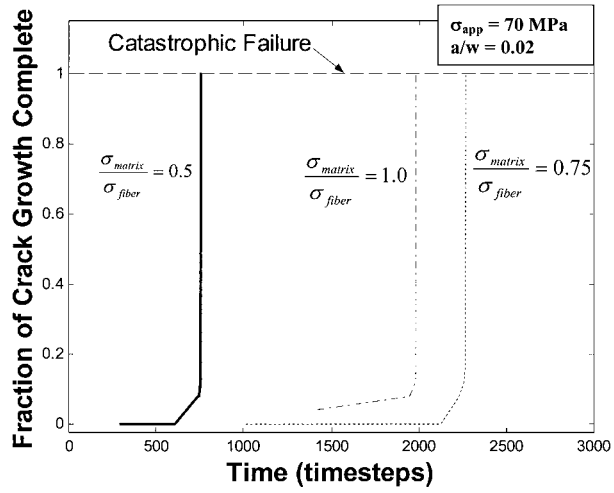

Figure 8 Typical results of macrocrack length as a function of time for matrix to fiber strength ratios of 0.05, 0.75, and 1.0. The initial macrocrack length to specimen width ratio was 0.02 and the applied stress was 70 MPa in each case.

dominated by the random variation of mini-composite behavior for mini-composite elements away from the macrocrack tip, and dominated by the magnitude of the stress gradient near the macrocrack tip. For smaller values of the matrix to fiber strength ratio, the predicted creep lifetime response surface exhibited significant topography. The predicted creep lifetime of neighboring mini-composite elements was dominated by mini-composite element orientation within the zone of stress concentration, and a combined function of mini-composite element orientation and random variability outside the zone of significant stress concentration.

Fig. 8 shows the typical relationship between macrocrack length and relative time for an initial crack length to specimen width ratio of 0.02 and three values of matrix to fiber strength ratios, 1.0, 0.75, and 0.5. At a matrix to fiber strength ratio of 1.0, accumulation of creep damage resulted in macrocrack extension due to failure of highly stressed mini-composite elements in the zone of significant stress concentration. It was observed that the first 75% of the life was required to accumulate enough creep damage in these highly stressed mini-composite elements to initiate macrocrack extension. Macrocrack growth continued slowly by failure of mini-composite elements at the macrocrack tip in the absence of microcrack formation away from the macrocrack tip, and macrocrack extension resulted in significant acceleration of creep damage accumulation in elements near the macrocrack tip due to stress redistribution associated with crack growth. After the macrocrack had grown approximately 10% of the distance across the composite, microcracks began to form in both 0° and 90° mini-composite elements. Macrocrack extension accelerated dramatically at this point due to macrocrack growth by connection of microcracks, and the transition to rapid macrocrack extension occurred after about 95% of the predicted creep life.

At a matrix to fiber strength ratio of 0.5, accumulation of creep damage initiated with failure of highly stressed 90° mini-composite elements in the zone of

significant stress concentration near the macrocrack tip. Since these 90° mini-composite elements exhibited significantly lower critical stresses than 0° mini-composite elements, microcrack formation was constrained to the 90° mini-composite elements. Macrocrack extension initiated and proceeded by connection of microcracks formed in 90° mini-composite elements. No macrocrack extension was observed for the first 85% of the life, and then transition to rapid macrocrack extension by connection of microcracks in 90° mini-composite elements resulted in catastrophic failure. Since the 90° mini-composite elements had significantly lower predicted creep lifetime and macrocrack extension occurred by connection of these elements, a significantly lower creep lifetime was predicted for the composite due to formation of a regular array of microcracked 90° mini-composite elements.

At a matrix to fiber strength ratio of 0.75, there was less disparity between the predicted creep lifetime of 0° and 90° mini-composite elements within the zone of significant stress concentration near the macrocrack tip. Creep damage initiated with failure of highly stressed 90° mini-composite elements near the macrocrack tip in a manner similar to that observed for a matrix to fiber strength ratio of 0.5. However, due to the higher critical strength of these elements for a matrix to fiber strength ratio of 0.75, compared to a matrix to fiber strength ratio of 0.5, longer times were required to initiate damage. The strong local effect of force distribution from failed mini-composite elements help constrain creep damage to microcrack formation in 90° mini-composite elements near the site of initial microcrack formation. Eventually, macrocrack extension occurred by connection of microcracked 90° mini-composite elements, but onset of macrocrack extension was offset until approximately 95% of the predicted creep life had passed. Once macrocrack extension started, stress redistribution associated with macrocrack growth resulted in the rapid acceleration of creep damage accumulation followed by the onset of catastrophic failure in a manner similar to that observed for a matrix to fiber strength ratio of 1.0.

The primary effect of weakening the 90° mini-composite elements with a reduction of matrix to fiber strength ratio from 1.0 to 0.75 was the delayed onset of macrocrack extension. This delayed onset of macrocrack extension delayed the rapid acceleration of creep damage in mini-composite elements at the macrocrack tip due to stress redistribution associated with macrocrack growth. In essence, the formation of microcracks slightly away from the macrocrack tip combined with the strong local effect of force redistribution from microcracked mini-composite elements effectively shielded the mini-composite elements at the macrocrack tip from acceleration of creep damage accumulation. If the 90° mini-composite elements were weakened too much, i.e. matrix to fiber strength ratio of 0.5, premature onset of microcrack formation and macrocrack extension were predicted.

The effect of shielding mini-composite elements at the macrocrack tip from accelerated creep damage accumulation at a matrix to fiber strength ratio of 0.75 was still evident as the applied stress was increased from 70 to 125 MPa as shown in Fig. 7a. However, the effect of increased initial macrocrack length from 0.02 to 0.05 resulted in a strong localization of the creep damage to the elements at the macrocrack tip. Therefore, shielding of mini-composite elements at the macrocrack tip from accelerated creep damage accumulation due to microcrack formation was not effective when the matrix to fiber strength ratio was reduced to 0.75 with an initial macrocrack length to specimen width ratio of 0.05 or 0.10 as shown in Fig. 7b.

4. Conclusions

A Monte Carlo model of creep crack growth in a 0°/90° plain-weave ceramic-grade Nicalon fiber reinforced SiC composite lamina containing an edge crack loaded in Mode I has been developed. The composite was modeled as alternating 0° and 90° mini-composite elements. The 0° mini-composite elements contained a ceramic-grade Nicalon fiber tow oriented parallel to the applied stress. The 90° mini-composite elements contained a ceramic-grade Nicalon fiber tow oriented perpendicular to the applied stress. The unit dimension of each mini-composite element was equal to the width of a fiber tow.

The Monte Carlo model utilized the behavior of individual fiber tows to predict the response of individual mini-composite elements in the woven composite lamina using a power-law relationship between mini-composite element lifetime and local stress. The local stress was computed using the well-known Linear Elastic Fracture Mechanics solution to the stress field surrounding a sharp edge crack. Failure modes of both 0° and 90° mini-composite elements included tensile failure of fibers, tensile failure of the matrix, and shear failure of the tow interface. Material variability of constituent phases was incorporated into the Monte Carlo model using a random Gaussian variation of the predicted creep lifetime of each mini-composite element. The mean of the Gaussian distribution was the power-law prediction of the time required to observe the most critical type of failure for each mini-composite element, and the standard deviation of the Gaussian distribution was taken as 7.5% of the mean value.

The model permitted macrocrack extension by failure of mini-composite elements adjacent to the macrocrack tip, and microcrack formation by failure of mini-composite elements not adjacent to the macrocrack tip. Once a mini-composite element had failed, force from that failed mini-composite element was distributed to remaining mini-composite elements. Force distribution was accomplished by re-computing the Linear Elastic Fracture Mechanics stress field if macrocrack extension was predicted. Force distribution was accomplished by an inverse square redistribution law if microcrack formation was predicted. Macrocrack extension by connection of microcracks as appropriate was also permitted.

Catastrophic failure was defined as macrocrack extension to an edge of the composite lamina. Stress dependent power-law behavior in the woven composite

lamina was predicted from creep degradation of fibers, and a power-law exponent of 3.1 ± 0.1 was predicted. Failure in 0° mini-composite elements was predicted to occur by tensile failure of fibers. Failure in 90° mini-composite elements was predicted to occur by tensile failure of the matrix. Matrix failure in 90° mini-composite elements was thought to be equivalent to the physical process of delamination cracking.

Critical parameters in prediction of composite lamina behavior were applied stress, initial macrocrack length, and the matrix to fiber strength ratio. Increased applied stress and increased initial macrocrack length resulted in lower predicted creep lifetime. For small initial macrocrack length, a reduction of the matrix to fiber strength ratio to 0.75 was predicted to increase the creep lifetime by about 10%. This improvement in the creep lifetime was thought to be related to the formation of microcracks in the 90° mini-composite elements, and shielding of elements at the macrocrack tip from rapidly accelerating creep damage due to stress redistribution. This shielding effect was predicted for all levels of applied stress investigated. For larger values of initial macrocrack length, decreased creep lifetime was predicted for a decrease in the matrix to fiber strength ratio from 1.0 to 0.75. This observation suggests the shielding effect of microcrack formation in the 90° mini-composite elements was only effective at very small crack sizes. The predicted creep life decreased for decreased matrix to fiber strength ratios below 0.75 for all combinations of applied stress and initial macrocrack length investigated.

References

1. J. A. DICARLO, *J. Mat. Sci.* **21**(1) (1986) 217.
2. E. Y. SUN, S. T. LIN and J. J. BRENNAN, *J. Amer. Ceram. Soc.* **80**(3) (1996) 3065.
3. G. N. MORSCER, *ibid.* **80**(8) (1997) 2029.
4. M. J. VERILLI, A. M. CALOMINO and D. N. BREWER, "ASTM STP 1309," edited by M. G. Jenkins, S. T. Gonezy, E. Lara-Curzio, N. E. Ashbaugh and L. Zawada (ASTM, Philadelphia, 1997) p. 156.
5. T. E. STEYER, F. W. ZOK and D. P. WALLS, *J. Amer. Ceram. Soc.* **81**(8) (1998) 2140.
6. J. W. CAO, M. MIZUNO, Y. NAGANO, Y. KAGAWA and H. KAYA, *Ceram. Sci. Eng. Proc.* **19**(3) (1999) 251.
7. S. Q. GUO, Y. KAGAWA, M. TAKEDA, H. ICHIKAWA, M. FUJIKURA and R. JANAKA, *ibid.* **20**(3) (1999) 625.
8. M. ANDO, H. SERIZAWA and H. MURAKAWA, *ibid.* **21**(3) (2000) 195.
9. C. A. LEWINSOHN, C. H. HENAGER and R. A. JONES, *ibid.* **21**(3) (2000) 415.
10. M. MIZUNO, S. ZHU and Y. KAGAWA, *ibid.* **21**(3) (2000) 433.
11. A. SAEKI, M. TAKEDA, A. YOKOYAMA and T. YOSHIDA, *ibid.* **21**(3) (2000) 363.
12. F. MACDONALD and D. N. COON, *J. Mat. Sci.* **36** (2001) 1681.
13. P. SODANAPALLI and D. N. COON, *ibid.* **37** (2002) 1.
14. *Idem.*, *ibid.* **37** (2002) 4197.
15. L. P. ZAWADA, L. M. BUTKUS and G. A. HARTMAN, *J. Amer. Ceram. Soc.* **74**(11) (1991) 2858.
16. S. RAGHURAMAN, J. F. STUBBINS, M. K. FERBER and A. A. WERESZCZAK, *J. Nuc. Mat.* **212–215** (1994) 840.
17. P. REYNAUD, D. ROUBY, G. FANTOZZI, F. ABBE and P. PERES, *Ceram. Trans.* **57** (1995) 95.
18. E. LARA-CURZIO, *J. Amer. Ceram. Soc.* **80**(12) (1997) 3268.
19. F. W. HURWITZ, A. M. CALOMINO and T. R. McCUE, *Ceram. Sci. Eng. Proc.* **20**(3) (1999) 25.
20. D. N. COON and A. MOTKUR, *J. Mat. Sci.* **35** (2000) 3207.
21. L. A. GIANNUZZI and C. A. LEWINSOHN, *Ceram. Sci. Eng. Proc.* **21**(3) (2000) 469.
22. G. N. MORSCHER, *ibid.* **21**(3) (2000) 423.
23. G. N. MORSCHER, J. HURST and D. BREWER, *J. Amer. Ceram. Soc.* **86**(6) (2000) 1441.
24. L. U. J. T. OGBUJI, *Ceram. Sci. Eng. Proc.* **21**(3) (2000) 477.
25. D. N. COON and A. M. CALOMINO, *J. Mat. Sci.* **36** (2001) 2597.
26. J. W. HOLMES, *ibid.* **26** (1991) 1808.
27. N. I. IYENGAR and W. A. CURTIN, *Acta Materialia* **45** (1997) 1489.
28. G. N. MORSCHER and J. Z. GYELLENYESI, *Ceram. Sci. Eng. Proc.* **19**(3) (1998) 241.
29. T. L. ANDERSON, "Fracture Mechanics—Fundamentals and Applications," 2nd ed. (CRC Press, 1995) p. 112.
30. W. P. KEITH and K. T. KEDWARD, *J. Amer. Ceram. Soc.* **80**(2) (1997) 357.

Received 30 January 2002
and accepted 6 May 2003